ELSEVIER

10 December 2001

Physics Letters A 291 (2001) 226–231

PHYSICS LETTERS A

www.elsevier.com/locate/pla

Theory and experiment for ultrahigh pressure shock Hugoniots

Balazs F. Rozsnyai *, James R. Albritton, David A. Young, Vijay N. Sonnad, David A. Liberman

Lawrence Livermore National Laboratory, Livermore, CA 94550, USA

Received 3 August 2001; accepted 4 October 2001
Communicated by A.R. Bishop

Abstract

Several equation of state models for hot, dense matter are compared with experimental data for the shock Hugoniots of beryllium, aluminum, iron, copper, and molybdenum up to extreme pressures. The best models are in good agreement with experiment and with one another, suggesting that our understanding of dense, partially ionized matter is good. © 2001 Published by Elsevier Science B.V.

PACS: 05.20.Jj; 05.70.Ce; 31.15.Ar; 31.15.Bs; 51.30.+i; 62.50.+p
Keywords: Equation of state; Shock Hugoniot; Ionization

1. Introduction

When matter is subjected to a strong shock wave the shocked material is heated, becomes partially or completely ionized, and in the case of an extremely strong shock the density approaches the ideal gas limit of $\rho = 4\rho_0$, where ρ_0 is the initial density [1]. The collection of the pressure–density points of the shocked material, or Hugoniot, depends on the details of the equation of state (EOS) of the matter. At intermediate shock pressures when the material becomes partially ionized, the Hugoniot will depend on the precise quantum-mechanical state of the matter. Thus the theoretical estimation of Hugoniots is part of the problem of understanding the physics of hot, dense matter. Comparisons of theoretical and experimental shock Hugoniots in the partial ionization region have been published in the past [2–4], but only for a limited range of materials and theoretical models. In this Letter we make comparisons for a wider range of atomic number and for rather different EOS models. Our objective is to determine how accurately the present set of EOS models agrees with experiment and how the models agree with one another.

New experimental methods, including the Sandia Z machine [5] and high-powered lasers [6] have the potential to generate shocks above 10 Mbar, and in the case of the National Ignition Facility at Livermore, above 100 Mbar [7]. In anticipation of new shock data in the regime of strong electronic excitation, we here re-examine the theoretical predictions of the present generation of EOS models.

2. Models

Theoretical EOS models valid for ionization states must include accurate descriptions of atomic structure. The simplest ionization model is the Saha model [8],

* Corresponding author.
E-mail address: rozsnyai1@llnl.gov (B.F. Rozsnyai).

0375-9601/01/$ – see front matter © 2001 Published by Elsevier Science B.V.
PII: S0375-9601(01)00661-2

which assumes a noninteracting ideal gas with ionization states given by the experimental values of the ionization potentials. The statistical mechanics of the equilibrium mixture of ions and electrons predicted by the Saha model is well understood and is useful in theoretical astrophysics. The Saha approximation can be systematically improved by adding electron–ion, ion–ion, and electron–electron Coulomb interactions, excited states, and corrections for degeneracy and liquid correlations [4].

Another approach is to compute the atomic total energies with quantum-mechanical self-consistent field methods [9,10]. The atomic boundary conditions must reflect the condensed-matter state and the excited state energy levels are populated according to a Fermi distribution at nonzero temperatures. This is an average-atom model that includes all excitation and ionization states in a single model atom. The simplest average-atom model is the semiclassical Thomas–Fermi model [11]. Thomas–Fermi accurately represents the high density and high temperature limits of matter, and it can be systematically improved with exchange and quantum terms. Solving the Schrödinger or Dirac equation self-consistently in the one-electron local-density approximation gives a more realistic model of the atom. Each model type makes strategic approximations that ultimately must be tested against experiment. We have generated shock Hugoniot curves with several different EOS models in order to compare them with experimental data and with each other.

QEOS is a global equation of state model developed in the 1980's [12]. It started as an online subroutine for hydrodynamic codes, and it has evolved into a table generator for EOS data libraries. The QEOS model separates the thermodynamic functions into electronic and ionic parts. The electronic part is approximated by the Thomas–Fermi model, corrected by a volume-dependent bonding term which enforces the conditions $P = 0$, $E = 0$ at the reference density and temperature. The ionic part is composed of a Debye model for the solid, a Lindemann melting curve, and a soft-sphere model for the liquid. There is no volume discontinuity at the melting point in the QEOS model. QEOS has been modified to allow more accurate fitting of experimental data in the low-temperature region [13]. This includes fitting shock Hugoniots, isotherms, and liquid–vapor critical points. In general, QEOS is a good first approximation to a global EOS which gives good fits to the low-temperature EOS. The fundamental limitation of QEOS is its reliance on the simple Thomas–Fermi model, which overestimates the ionization of electrons, and leads to pressures along the Hugoniot which are too large.

ACTEX [4] is a plasma model based on an activity expansion of the grand partition function for a Coulomb gas of ions and electrons. The activity expansion is renormalized to produce terms representing the relevant ionic and atomic species in the plasma. ACTEX uses parameterized electron–ion potentials fitted to experimental spectroscopic data and has corrections for strong ion–ion coupling. ACTEX fails where the electron–ion coupling becomes strong, typically at temperatures below 10 eV.

HOPE [9,14] is a self-consistent Dirac–Slater average atom model and it can account for detailed electronic configurations. In HOPE the boundary conditions for the bound states are given at the ion-sphere radius requiring that either the wave function or its derivative be zero, thus giving a rough estimate for the widths of the electronic bands. The bound states in HOPE are normalized within the ion-sphere radius, which distinguishes it from the INFERNO model described below. The low and high-energy continuum states are separated and they are treated quantum mechanically and in the Thomas–Fermi model, respectively. The primary purpose of HOPE is to compute opacities, but since opacities require an accurate quantum mechanical basis, the EOS is an important part of the HOPE code.

INFERNO [10] is a model of an atom in a jellium plasma. The one-electron Dirac equation is solved self-consistently with the constraint that the atomic volume is electrically neutral. Exchange and correlation are included through the local density approximation. The atom will have bound states and a continuum. The continuum is treated in the same way as the bound states so that the transition from bound to continuum states is smooth, and resonant states are computed accurately. Since the atomic wave function can spread out beyond the cell boundary into the jellium, there is some arbitrariness in the separation of the atom from the jellium medium and in the calculation of the thermodynamic functions.

The next improved level of physics modeling is to solve the quantum mechanical problem of atoms in a

solid or liquid state at finite temperatures where partial ionization can occur. Warm dense matter (WDM) models include finite-temperature band structure models [15] and quantum molecular-dynamics models with electronic excitation [16]. These are local-density approximation models with finite-temperature exchange and correlation functionals. The WDM models are among the most realistic models of electronically excited dense matter.

3. Experimental data

Experimental Hugoniot data on Be [17–20], Al [21–27], Fe [17,21,28], Cu [17,21,27], and Mo [17,21,27, 29] have been collected for comparison with the EOS models discussed above. There are several experimental methods [30] that have been used for generating well-defined shock states, from low pressures in the tens of kilobars, to high pressures above 100 Mbar. At lower pressures, explosive-generated plane shock waves have been used. Two-stage gas guns have been used to generate pressures up to 5 Mbar. Explosive-driven spherical implosions and laser-driven plane waves can yield shocks in the 10 Mbar range. Underground nuclear explosions have been used for generating shocks up to 4000 Mbar. If the shocks have been measured accurately, superimposing all of these data should yield a single smooth shock Hugoniot curve.

The maximum pressures reached in the experiments are Be, 18 Mbar; Al, 4000 Mbar; Fe, 105 Mbar; Cu, 61 Mbar; and Mo, 40 Mbar. These ultrahigh pressure states lie well within the strongly excited regime where the thermal electron pressure is a significant part of the total pressure.

Laser and magnetically driven shocks have already begun to produce data in this regime, and we can expect a steady stream of new data above 10 Mbar. Once new data begin to accumulate, it will be necessary to test the best theoretical models for adequacy.

4. Computations and comparisons

We used the models described in Section 2 to compute shock Hugoniots from room temperature up to the full ionization temperature for the elements Be, Al, Fe, Cu, and Mo. The Hugoniot points were obtained from the EOS tables produced by each model by solving the equation

$$E - E_0 = (1/2)(P + P_0)(V_0 - V), \tag{1}$$

where E, P, and V are the internal energy per atom, pressure, and volume per atom, respectively. The subscript "0" refers to the initial state, which is at room temperature and 1 atm pressure. EOS tables were produced for a temperature–density grid and Eq. (1) was solved numerically for each isotherm in the table. The spacing of the grid points determines the resolution of details in the computed Hugoniots. For the QEOS and ACTEX models, accurate models of the ionic motion are included. For the HOPE and INFERNO models, the ions are assumed to be ideal gas particles. In Figs. 1–5 we show the comparisons between the theoretical and experimental Hugoniots.

All of the theories show density maxima in the range $5\rho_0$–$6\rho_0$. In this region the electrons from the ionic cores are being ionized. The shock density increases beyond the infinite pressure limit of $4\rho_0$ in the electron ionization region because ionization increases the heat capacity without a corresponding pressure increase. As ionization is completed, the plasma approaches an ideal gas of nuclei and electrons and the density approaches $4\rho_0$.

QEOS shows no structure in the ionization region because it is based on the Thomas–Fermi statistical theory, which has no electron shell structure. ACTEX, HOPE, and INFERNO do show oscillations in the density because the successive electron shells are accurately represented and are ionized as kT reaches the ionization potentials of each electron shell.

For Be, the ACTEX, HOPE, and INFERNO predictions show a single density maximum, corresponding to the ionization of the K electron shell. The three predicted shock curves in the density maximum region are in good agreement. QEOS predicts higher pressures and a lower density maximum. The two WDM calculations are done with finite-temperature plane-wave electron band theory plus ideal gas ions. The two cases shown use the $T = 0$ and the finite-temperature exchange–correlation functionals. The finite-temperature exchange–correlation results appear to be too low in pressure. All of the other models come into good agreement with experiment in the 10 Mbar region.

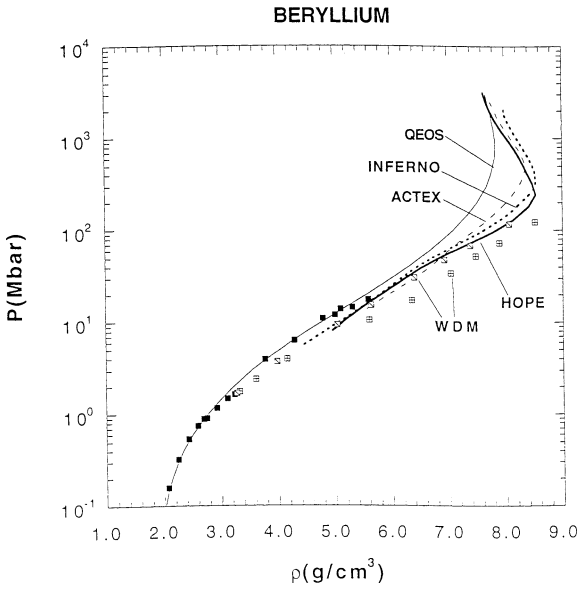

Fig. 1. Beryllium Hugoniots. Experimental data are black squares. The high-temperature band structure (WDM) points are given by squares with diagonal ($T = 0$ exchange–correlation) and squares with cross ($T > 0$ exchange–correlation).

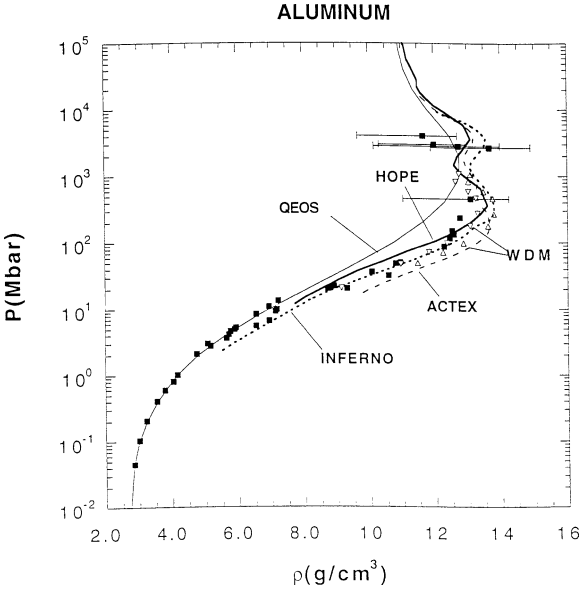

Fig. 2. Aluminum Hugoniots. Experimental data are black squares. The quantum molecular dynamics data (WDM) are open inverted triangles ($T = 0$ exchange–correlation) and open triangles ($T > 0$ exchange–correlation).

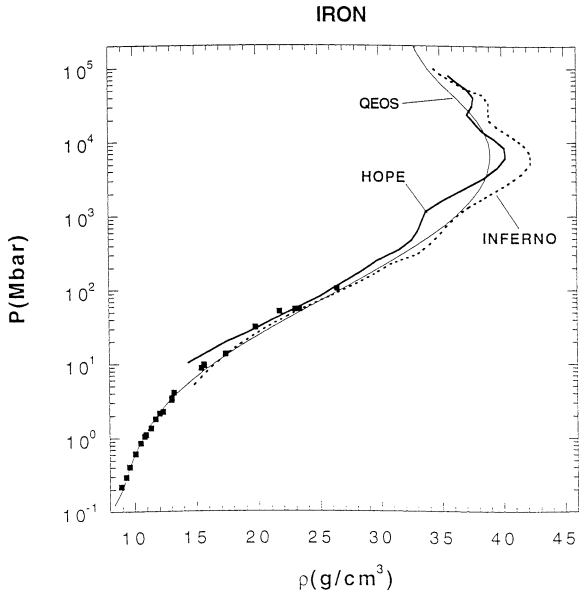

Fig. 3. Iron Hugoniots. Experimental data are black squares.

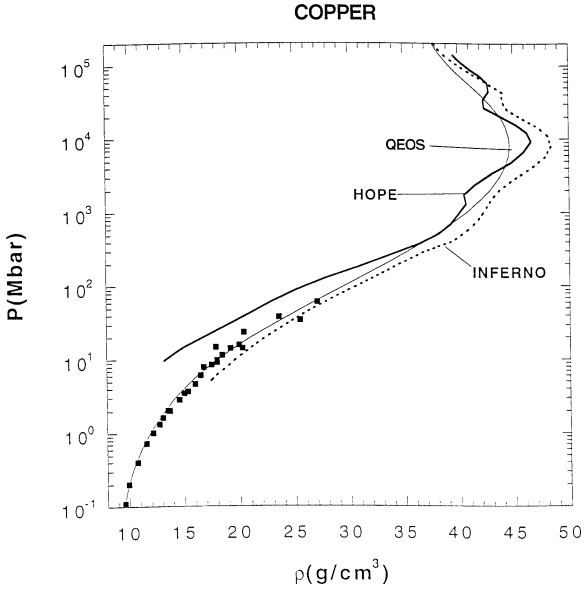

Fig. 4. Copper Hugoniots. Experimental data are black squares.

For Al, there are two density maxima corresponding to the K and L electron shells. Again, ACTEX, HOPE, and INFERNO are in good agreement in predicting the density maxima. Comparison of the QEOS data with previous three serves as a good example to

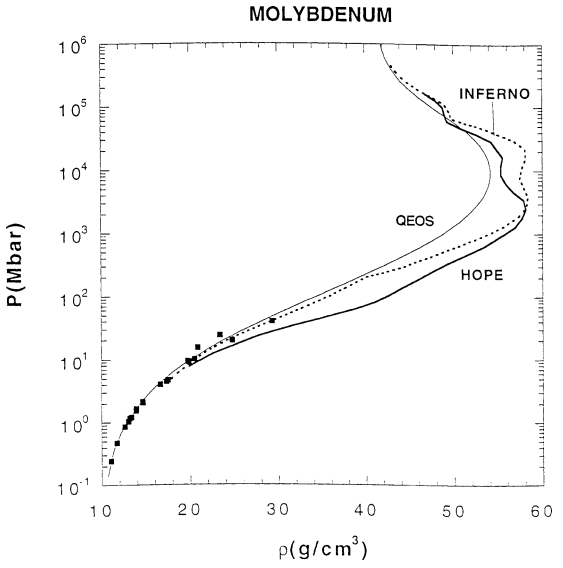

Fig. 5. Molybdenum Hugoniots. Experimental data are black squares.

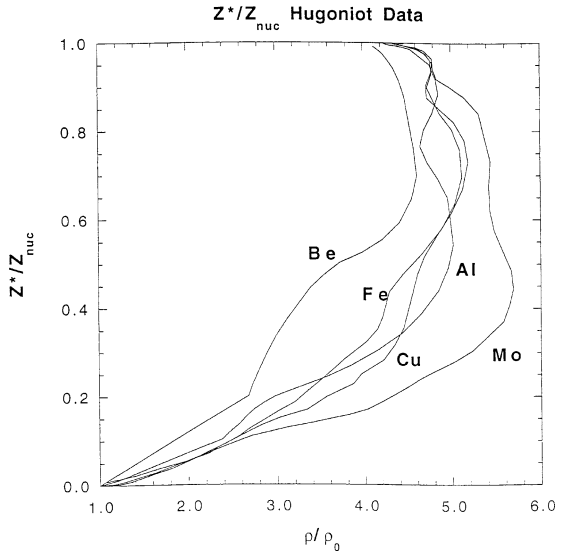

Fig. 6. HOPE values of Z^*/Z_{nuc} along the Hugoniots of Be, Al, Fe, Cu, and Mo, plotted against the density ratio ρ/ρ_0.

demonstrate the effect of the presence or absence of electron shells. QEOS does not have oscillations due to the ionization of the L and K shells, since electron shell structure is not included in the Thomas–Fermi model. The QEOS Hugoniot shows lower densities than the ACTEX, HOPE and INFERNO Hugoniots and consequently, the QEOS pressures are higher before the L shell ionization and lower before the K-shell ionization. Similar results hold for Figs. 3–5. The WDM models are based on quantum molecular dynamics with $T = 0$ and finite-temperature exchange–correlation functionals. The WDM models were only taken to the lower density maximum, but they agree well with the other models. Al is the one case where experimental data are available over the whole range of shock ionization. Although the experimental errors at the highest pressures are large, the data are consistent with the best theory.

For Fe and Cu there are three density maxima or inflections corresponding to the K, L, and M electron shells. The L shell ionization feature gives the largest density increase. The disagreement between HOPE and INFERNO is now larger than for Al, and HOPE actually overlaps the QEOS results. For Mo, there are three density inflections or maxima corresponding to the K, L, and M shells, and a rather weak feature near 40 g/cm^3, which apparently corresponds to the N shell. The disagreements between HOPE and INFERNO in this lower-pressure region are now very noticeable. For these three elements, INFERNO gives better agreement with experimental data, and gives perhaps the best prediction of future shock experiments.

The degree of ionization Z^*/Z_{nuc} and the temperature along the Hugoniot are useful variables that the EOS codes can compute. These variables are computed with the HOPE code and are plotted against the reduced variable ρ/ρ_0 in Figs. 6 and 7. Fig. 6 shows that the starting slopes of Z^*/Z_{nuc} decrease with increasing nuclear charge. We attribute that to the fact that at low temperatures the Z^*'s differ only slightly due to the different ionization energies of the top levels, thus the division by Z_{nuc} yields smaller numbers for the heavier elements. It is interesting that the maximum shock compression appears to increase with Z_{nuc}, but we do not have an explanation of this at present.

In summary, the good agreement of the quantum-mechanical EOS models with experiment and with each other for Be and Al in the region of high ionization suggest that accurate predictions of the EOS are possible. We hope that with the forthcoming National Ignition Facility laser, more high temperature experimental data will be available for the heavier elements.

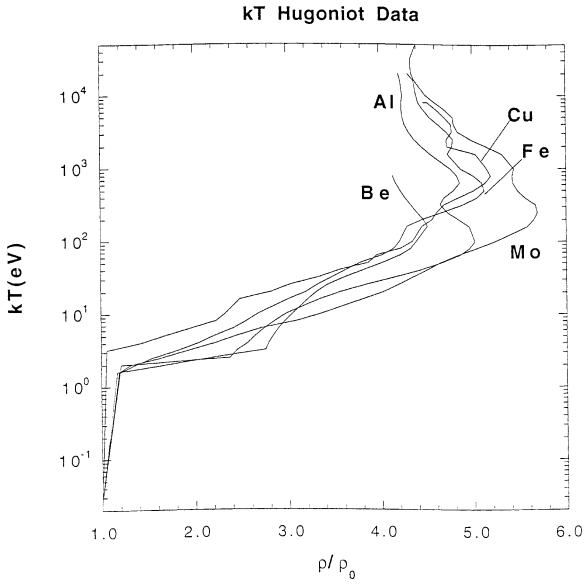

Fig. 7. HOPE values of shock temperature (in eV) for Be, Al, Fe, Cu, and Mo, plotted against the density ratio ρ/ρ_0.

Acknowledgements

This work was performed under the auspices of the U.S. Department of Energy by University of California Lawrence Livermore National Laboratory under contract No. W-7405-Eng-48. We thank T.W. Barbee III and M.P. Surh for release of their WDM data prior to publication.

References

[1] Ya.B. Zel'dovich, Yu.P. Raizer, Physics of Shock Waves and High-Temperature Hydrodynamic Phenomena, Vol. 1, Academic Press, New York, 1966, Chapter 3.
[2] D.A. Young, J.K. Wolford, F.J. Rogers, K.S. Holian, Phys. Lett. 108A (1985) 157.
[3] E.N. Avrorin, B.K. Vodolaga, V.A. Simonenko, V.E. Fortov, Usp. Fiz. Nauk 163 (1993) 1, Phys. Usp. 36 (1993) 337.
[4] F.J. Rogers, D.A. Young, Phys. Rev. E 56 (1997) 5876.
[5] C.A. Hall, J.R. Asay, W.M. Trott, M. Knudson, K.J. Fleming, M.A. Bernard, B.F. Clark, A. Hauer, G. Kyrala, in: M.D. Furnish, L.C. Chhabildas, R.S. Hixson (Eds.), Shock Compression of Condensed Matter—1999, American Institute of Physics, Melville, NY, 2000.
[6] L.B. DaSilva, P. Celliers, G.W. Collins, K.S. Budil, N.C. Holmes, T.W. Barbee Jr., B.A. Hammel, J.D. Kilkenny, R.J. Wallace, M. Ross, R. Cauble, A. Ng, G. Chiu, Phys. Rev. Lett. 78 (1997) 483.
[7] G. Collins, personal communication.
[8] S. Eliezer, A. Ghatak, H. Hora, An Introduction to Equations of State: Theory and Applications, Cambridge University Press, Cambridge, 1986, Chapter 7.
[9] B.F. Rozsnyai, Phys. Rev. A 5 (1972) 1137.
[10] D.A. Liberman, Phys. Rev. B 20 (1979) 4981.
[11] S. Eliezer, A. Ghatak, H. Hora, An Introduction to Equations of State: Theory and Applications, Cambridge University Press, Cambridge, 1986, Chapter 9.
[12] R.M. More, K.H. Warren, D.A. Young, G.B. Zimmerman, Phys. Fluids 31 (1988) 3059.
[13] D.A. Young, E.M. Corey, J. Appl. Phys. 78 (1995) 3748.
[14] A. Goldberg, B.F. Rozsnyai, P. Thompson, Phys. Rev. A 34 (1986) 421.
[15] T.W. Barbee III, personal communication.
[16] M.P. Surh, T.W. Barbee III, L.H. Yang, Phys. Rev. Lett. 86 (2001) 5958.
[17] S.P. Marsh, LASL Hugoniot Data, University of California Press, Berkeley, 1980.
[18] W.M. Isbell, F.H. Shipman, A.H. Jones, General Motors Corp. Materials Science Laboratory Report MSL-68-13, 1968.
[19] W.J. Nellis, J.A. Moriarty, A.C. Mitchell, N.C. Holmes, J. Appl. Phys. 82 (1997) 2225.
[20] C.E. Ragan III, Phys. Rev. A 25 (1982) 3360.
[21] A.V. Bushman, I.V. Lomonosov, V.E. Fortov, Equations of State for Metals at High Energy Density, Institute of Chemical Physics, Chernogolovka, 1992, in Russian.
[22] V.A. Simonenko, N.P. Voloshin, A.S. Vladimirov, A.P. Nagibin, V.N. Nogin, V.A. Popov, V.A. Vasilenko, Yu.A. Shoidin, Zh. Eksp. Teor. Fiz. 88 (1985) 1452, Sov. Phys. JETP 61 (1985) 869.
[23] A.P. Volkov, N.P. Voloshin, A.S. Vladimirov, N.N. Nogin, V.A. Simonenko, Pis'ma Zh. Eksp. Teor. Fiz. 31 (1980) 623, JETP Lett. 31 (1980) 588.
[24] E.N. Avrorin, B.K. Vodolaga, N.P. Voloshin, V.F. Kuropatenko, G.V. Kovalenko, V.A. Simonenko, B.T. Chernovolyuk, Pis'ma Zh. Eksp. Teor. Fiz. 43 (1986) 241, JETP Lett. 43 (1986) 309.
[25] A.S. Vladimirov, N.P. Voloshin, V.N. Nogin, A.V. Petrovtsev, V.A. Simonenko, Pis'ma Zh. Eksp. Teor. Fiz. 39 (1984) 69, JETP Lett. 39 (1984) 82.
[26] L.V. Al'tshuler, N.N. Kalitkin, L.V. Kuz'mina, B.S. Chekin, Zh. Eksp. Teor. Fiz. 72 (1977) 317, Sov. Phys. JETP 45 (1977) 167.
[27] A.C. Mitchell, W.J. Nellis, J.A. Moriarty, R.A. Heinle, N.C. Holmes, R.E. Tipton, G.W. Repp, J. Appl. Phys. 69 (1991) 2981.
[28] R.F. Trunin, M.A. Podurets, L.V. Popov, B.N. Moiseev, G.V. Simakov, A.G. Sevast'yanov, Zh. Eksp. Teor. Fiz. 103 (1993) 2189, JETP 76 (1993) 1095.
[29] R.S. Hixson, J.N. Fritz, J. Appl. Phys. 71 (1991) 1721.
[30] R.F. Trunin, Shock Compression of Condensed Materials, Cambridge University Press, Cambridge, 1998.